Identification of *Arabidopsis thaliana* phloem RNAs provides a search criterion for phloem-based transcripts hidden in complex datasets of microarray experiments

Rosalia Deeken[1,†], Peter Ache[1,†], Inga Kajahn[2], Joern Klinkenberg[1], Gerhard Bringmann[2] and Rainer Hedrich[1,*]

[1]*University of Würzburg, Julius-von-Sachs-Institute for Biosciences, Julius-von-Sachs-Platz 2, D-97082 Würzburg, Germany, and*
[2]*University of Würzburg, Institute of Organic Chemistry, Am Hubland, D-97074 Würzburg, Germany*

Summary

Phloem-mobile signals play a major role in plant nutrition, development and communication. In the latter context, phloem-mobile RNAs have been associated with signalling between plant tissues. In this study, we focused on the identification of transcripts in the shoot phloem of the model plant *Arabidopsis thaliana*. To isolate transcripts expressed in phloem parenchyma cells and in companion cell–sieve element complexes, we used laser microdissection coupled to laser pressure catapulting (LMPC). Mobile transcripts in sieve elements were isolated from leaf phloem exudates. After optimization of sampling and fixation, RNA of high quality was isolated from both sources. The modifications to the RNA amplification procedure described here were well suited to production of RNA of sufficient yield and quality for microarray experiments. Microarrays hybridized with LMPC-derived phloem tissue or phloem sap RNA allowed differentiation between phloem-expressed and mobile transcript species. Using this set of phloem transcripts and comparing them with microarrays derived from databases of light, hormone and nutrient treatment experiments, we identified phloem-derived RNAs as mobile, potential long-distance signals. Our dataset thus provides a search criterion for phloem-based signals hidden in the complex datasets of microarray experiments. The availability of these comprehensive phloem transcript profiles will facilitate reverse-genetic studies and forward-genetic screens for phloem and long-distance RNA signalling mutants.

Keywords: Arabidopsis, phloem, exudate, laser microdissection, microarrays, metabolites.

Introduction

Plant cells and tissues are metabolically interconnected via plasmodesmata (short distances) and the phloem network (long distances). As expected for a flowing cytosol, which predominantly translocates transport sugars, sugar alcohols, nitrogen-rich amino acids and hormonal signals, the phloem sap comprises a characteristic blend (Deeken *et al.*, 2002; Karley *et al.*, 2002; Lohaus *et al.*, 2000; Pommerrenig *et al.*, 2007). The protein spectrum is also phloem-specific. It is enriched in proteins known to bind metals, and those involved in redox control, stress responses, Ca²⁺ and G-protein signalling, and flowering (Giavalisco *et al.*, 2006). In addition, peptides such as systemins convey information to the plant about ongoing insect or microbe attacks in distal

parts (Li *et al.*, 2006). As a result, the basic defence cocktail of the phloem sap (Walz *et al.*, 2004), containing β-glucosidases and glucosinolates, is enriched by additional chemical weapons (Mewis *et al.*, 2005). Glucosinolates also accumulate in the phloem cells adjacent to sieve elements in preparation for fast defence reactions (Koroleva *et al.*, 2000). In Arabidopsis, specialized phloem idioblasts, containing myrosinases, and glucosinolate-rich S-cells, are thought to comprise a two-component system of defence against herbivory (Husebye *et al.*, 2002). Plants are also able to cope with viral attacks. Silencing of viral RNA is associated with the movement of small mobile RNAs (Lough and Lucas, 2006; Oparka, 2005).

Based on the fact that several RNA species use this long-distance pathway (Ivashikina *et al.*, 2003; Kehr and Buhtz, 2008; Pommerrenig *et al.*, 2006; Vilaine *et al.*, 2003), it has been suggested that plants utilize mobile RNA to integrate biotic and abiotic interactions and even developmental processes (Aung *et al.*, 2006; Gentili and Huss-Danell, 2003; Lucas *et al.*, 2001; Nishimura *et al.*, 2002; Olsson *et al.*, 1989) at the whole-plant level (e.g. Haywood *et al.*, 2005). RNA-binding proteins were also found, which may form a transport complex with RNA (Yoo *et al.*, 2004). In fact, for some transcripts, even the encoded proteins were detected in phloem exudates (Corbesier *et al.*, 2007; Mathieu *et al.*, 2007). This finding initiated an ongoing discussion as to whether the RNA or protein is the carrier of the long-distance signal. Grafting experiments are an elegant way to demonstrate that proteins and RNAs that carry specific information are transported via the phloem (An *et al.*, 2004; Corbesier *et al.*, 2007; Turnbull *et al.*, 2002).

To identify genes required for long-distance RNA signalling, we performed genome-wide expression profiling of mRNAs isolated from Arabidopsis phloem tissue of inflorescence stalks and from leaf exudates. The successful isolation of phloem mRNA was verified by analysis of transcripts known to be vascular tissue-specific marker genes, as well as by determination of the phloem solute pattern. The reliability of the gene sets as tools for identifying new genes expressed in the phloem was supported by results from RT-PCR experiments. Transcript profiles of mobile RNAs (phloem sap) and those expressed in the phloem tissue were compared to a companion-cell EST collection (Ivashikina *et al.*, 2003). Examples of how to use the phloem database in order to explore so far uncharacterized phloem genes and to dissect complex networks associated with light, hormone and nutrient signalling are discussed.

Results

In recent years, laser microdissection (LMD) and laser microdissection coupled to pressure catapulting (LMPC) have been established to isolate small fragments from plant tissue of interest to study gene expression profiles (Asano *et al.*, 2002). A critical step in these techniques is prevention of RNA fragmentation, so that it is possible to obtain a high yield of full-length RNA. However, protocols involving cross-linking (aldehyde containing) or non-cross-linking (alcohol containing) fixation steps have shown contradictory results (Inada and Wildermuth, 2005; Kerk *et al.*, 2003; Nakazono *et al.*, 2003; Yu *et al.*, 2007). In our hands, neither of the methods published worked satisfactorily with phloem samples derived from the inflorescence stem of Arabidopsis. We were able to identify phloem-localized transcripts in LMPC samples of Arabidopsis phloem by RT-PCR (Ivashikina *et al.*, 2003), but, in contrast to the results described previously, the

RNA yield of Arabidopsis preparations was not sufficient for quantitative analyses. In addition, the required subsequent amplification of low-yield RNA led to extreme cDNA fragmentation and thus to unreliable real-time PCR results. For this reason, array data on LMD-derived Arabidopsis embryos (Casson *et al.*, 2005) were removed from the GENEVESTIGATOR database.

This problem was overcome by optimization of the LMPC technique with respect to tissue fixation, RNA clean-up and amplification, and cDNA synthesis. The protocol described below provides reproducible and reliable transcript profiling from minute amounts of plant tissues and cell collections. It was also successfully applied to other Arabidopsis tissues, poplar samples and tobacco cells (data not shown) and therefore appears to be suitable for general application.

Preparation of phloem tissue sections with LMPC

Embedding of plant material in paraffin usually involves incubation at 60°C for several days. Long-term exposure to high temperatures is accompanied by significant loss of RNA and paraffin degradation. To avoid this, we equipped an exsiccator with a device that, after heating (e.g. in a drying cabinet), kept the temperature constant during wax infiltration (Figure S1). As a result, embedding times and exposure at elevated temperatures were reduced and RNA yields increased remarkably. The best morphological preservation of paraffin-embedded microtome sections was achieved at low temperatures. Use of a standard cryo-microtome, however, led to poor morphological preservation of rigid plant tissues. Cooling the complete cutting unit of a conventional rotary microtome (Leica, http://www.leica-microsystems.com) generated perfect cutting conditions (Figure S2). Using our modified sectioning and LMPC protocol, loss of RNA was negligible. For high quality RNA extraction and amplification, we transferred approximately $5 \times 10^6 \ \mu m^2$ laser micro-dissected phloem sections (Figure 1) (Ivashikina *et al.*, 2003) into the appropriate extraction buffer.

High-quality RNA amplification of LMPC sections for microarray hybridizations

As LMPC-derived material does not yield enough RNA for complex expression analysis via microarrays, an amplification step was required. Unfortunately, several commercial amplification kits did not allow linear amplification or quantification by real-time PCR of our RNA-derived cDNA samples. We therefore modified the SMART mRNA amplification protocol (BD/Clontech, http://www.clontech.com), and succeeded in amplifying full-length mRNA from extremely small samples. The amplified RNA was tested by quantitative RT-PCR for the relative abundance of marker
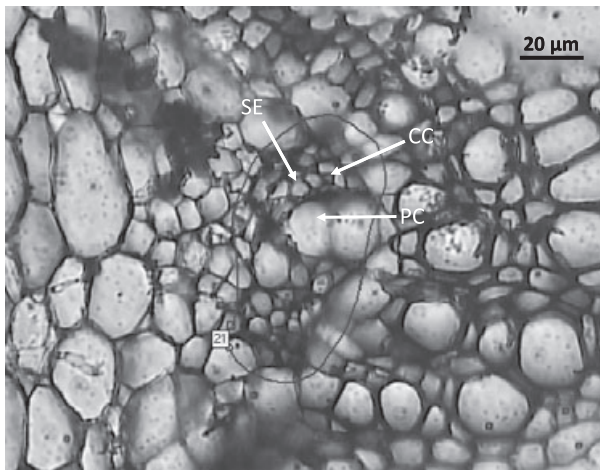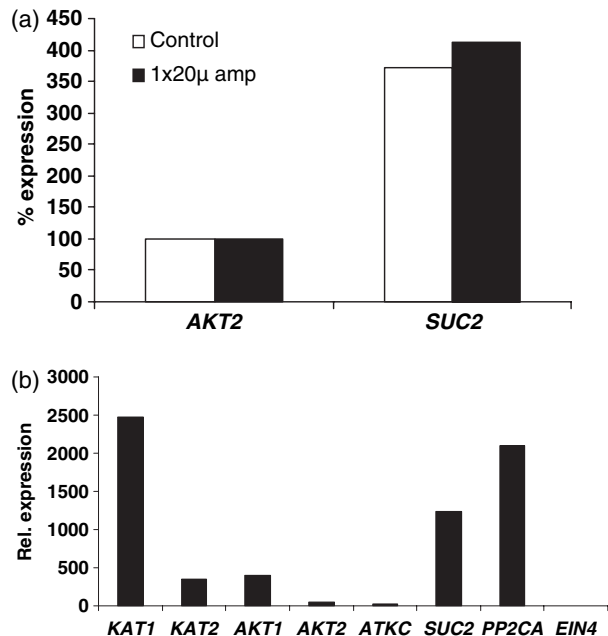
Figure 1. Cross-section of an Arabidopsis inflorescence stem with marked phloem region.
The laser cuts along the outlined margin. Due to the cutting width (approximately 5 μm), contamination of surrounding material is minimal. SE, sieve element; CC, companion cell; PC, parenchyma cell.

Figure 2. RNA amplification and marker transcripts in Arabidopsis LMPC samples.
(a) mRNA extracted from one 20 μm cross-section of an Arabidopsis inflorescence stem was amplified and compared to non-amplified mRNA of an inflorescence stem segment. Marker transcripts were determined by real-time PCR.
(b) Determination of transcript levels of known phloem genes in LMPC-samples revealed that, except for AKT2, all other transcript levels were comparable to those published by Ivashikina *et al.* (2003). EIN4 served as a negative control, because this transcript is not expressed in the phloem.

transcripts. For this purpose, we used the weakly expressed phloem K$^+$ channel *AKT2* (Marten *et al.*, 1999) and *SUC2*, a prominent sugar transporter of Arabidopsis companion cells (Imlau *et al.*, 1999). High-quality mRNA well suited for quantitative RT-PCR was amplified from as little as 2 ng starting material or ten single guard-cell protoplasts. In contrast to other amplification methods, neither the length nor the abundance of the tested transcripts affected the amplification result significantly (data not shown). Transcript numbers of non-amplified protoplast mRNA varied between samples. However, ratios between distinct transcripts appeared to be constant. This notion was supported by the amplification of RNA obtained from ten protoplasts (Figure 2a, black bars), which served as a further proof of the linearity of the amplification protocol. Furthermore, amplified RNA from one 20 μm section of paraffin-embedded Arabidopsis stem was compared with non-amplified RNA from 30 sections. The non-amplified sample revealed only one of the marker transcripts. In contrast, amplification of a single section resulted in values similar to those obtained from complete inflorescence stems (Figure 2a). LMPC-derived phloem samples were characterized by the presence of transcripts known to be expressed in the phloem (Figure 2b; Ivashikina *et al.*, 2003).

Before amplification, the isolated mRNA of LMPC sections was analysed in a Bioanalyzer (Agilent, http://www.home.agilent.com) and compared with amplified RNA. No significant difference in length distributions between the starting RNA material and amplified RNA was observed (Figure 3). In phloem LMPC samples, however, we found an accumulation of smaller transcripts (peak at 200 bp, Figure 3, right) compared to the cross-section control samples (peak at

1000 bp, Figure 3, left). The amplified LMPC-derived mRNA samples were then used to hybridize Affymetrix 22K microarrays (ATH1) (Affymetrix, http://www.affymetrix.com) in order to identify Arabidopsis phloem tissue-specific transcripts at the whole-genome level.

Collection of phloem exudate from Arabidopsis leaves

In order to identify transcripts that are mobile in the companion cell–sieve tube complex and therefore can traffic between different organs as a signal, leaf phloem exudates were harvested. EDTA stimulates phloem exudation by chelating Ca^{2+} and thereby prevents the formation of callose, which would seal sieve tubes after wounding (Wolf *et al.*, 1990). Leaves from adult rosette plants, just about to start flowering, were cut and the petiole was mounted into the 3 mm wide slit of a sampling cuvette (Figure 4a). The chamber, loaded with petioles of 50–70 leaves, was extensively washed with a large volume of sterile EDTA buffer to remove contaminations (Figure 4b). The EDTA buffer was adjusted to the osmotic potential of the petiole cells by addition of sorbitol to avoid swelling and subsequent bursting of cells at the cut

Figure 3. Quality control for RNA prior to and after RNA amplification.
The distribution of fragment length of the samples did not change as a result of the amplification procedure. LMPC-derived samples (right) were shifted towards smaller RNAs compared to total cross-sections (left). cs, cross-section; nt, nucleotide length in base pairs; FU, fluorescence units.
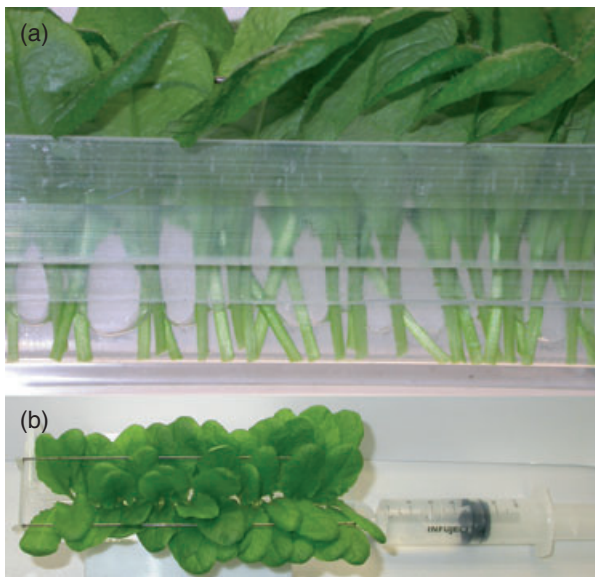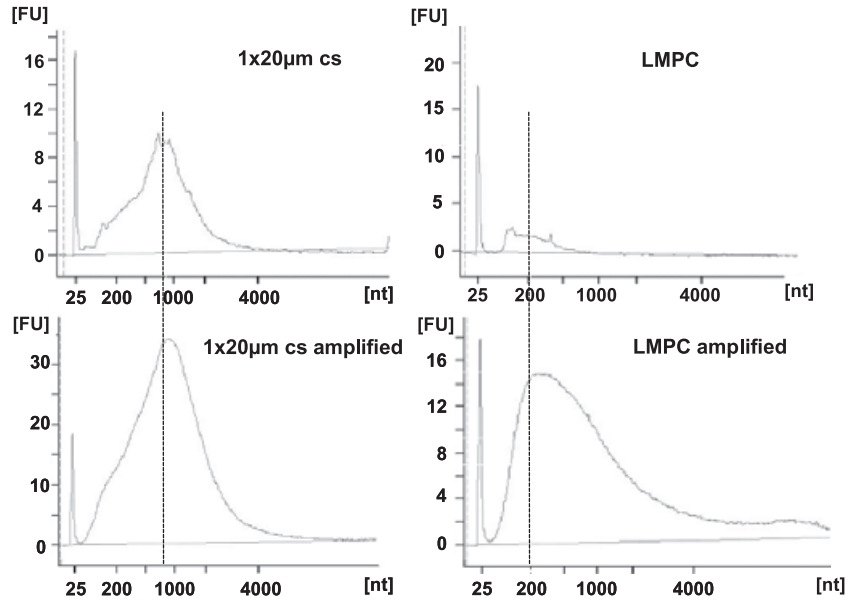
Figure 4. Device for phloem exudate collection from Arabidopsis leaves.
(a) Front view showing the position of petioles in the incubation slit covered by EDTA buffer solution.
(b) A syringe is connected to the device for washing the chamber and harvesting the samples (side view).

surface. During phloem sap exudation, the leaves were illuminated and incubated in CO_2- and H_2O-saturated air in an incubation chamber. This treatment induced closure of stomata, impeded transpiration and avoided the uptake and distribution of EDTA buffer via the xylem which would lead to the weakening of cell walls due to EDTA chelation of calcium. After phloem bleeding for 1 h, the buffer solution, which contained diluted phloem sap, was used for analyses of metabolite and mRNA compositions.

Verification of the nature of the leaf exudate

The origin of the exudate was analysed by determination of the sugar, amino acid and mineral content, as well as marker transcripts known to be localized in the phloem. Exudates were dominated by sucrose (96 ± 39 nmol g^{-1} FW), but mannitol, glucose and fructose contents were very low (Figure S3a). Among the amino acids, glutamate and glutamine represented the largest fraction (Figure S3b). Potassium was the major mineral found in these leaf exudates (Figure S3c).

The glucosinolate pattern of leaf extracts from *Arabidopsis thaliana* Col-0 was determined by utilizing the CE-ESI-oTOF-MS method, recently developed for glucosinolate analysis (Bringmann *et al.*, 2005). Further refinements of the method were necessary with regard to the analysis of small quantities of phloem exudates (see Experimental procedures). Glucosinolates are known to be phloem-mobile, of which the Arabidopsis phloem sap, in agreement with previous results (Chen *et al.*, 2001), contained the methoxyindol-3-ylmethyl glucosinolate exclusively (Figure 5).

In addition to the detection of phloem metabolites, the phloem exudates were also tested for contamination by transcripts from damaged cells of the cut petiole surface, such as mesophyll or epidermal cells. Transcripts of the mesophyll cell-specific molecular marker chloroplastic anhydrase (At3g01500) and the epidermal cell-specific marker very-long-chain fatty acid-condensing enzyme CUT1 (At1g68530) were used for amplification by RT-PCR (Inada and Wildermuth, 2005). Neither transcript was amplified from the phloem exudate by 40 PCR cycles, but actin2/8 and the sieve tube-specific copper chaperone CCH (At3g56240, Mira *et al.*, 2001) were amplified with this number of PCR cycles in
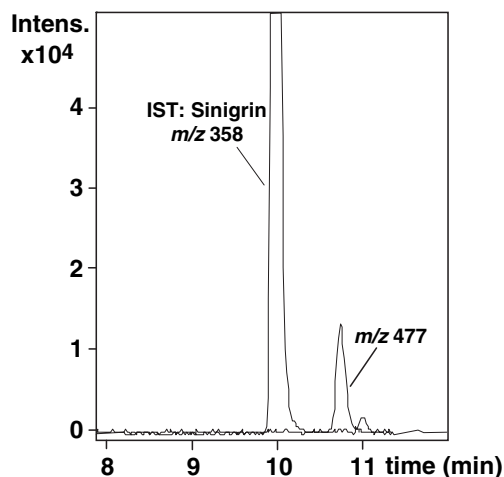
Figure 5. Phloem glucosinolate.
Electropherogram of an Arabidopsis phloem exudate, showing that methoxyindol-3-ylmethyl glucosinolate (m/z 477) is the only glucosinolate found in the phloem sap. The internal standard (IST) was sinigrin.

the same samples (Figure S4). This led us to conclude that contamination with RNA from damaged cells was negligible.

Taken together, this solute pattern is typical of the phloem sap of higher plants, indicating that the EDTA chelation technique is well suited to obtaining phloem sap from Arabidopsis leaves under the mildest possible conditions yet achieved.

Microarray analyses of phloem exudate and LMPC tissue samples

Hybridization and quality control of microarrays (ATH1; Affymetrix) as well as analysis of the data were performed at the Microarray Facility, University of Tübingen, Germany. The mRNA of four independent bleeding experiments was pooled and amplified by two cycles. Three mRNA pools of phloem exudate and another three of LMPC-derived phloem tissue were used for hybridization of three microarrays. The quality of the hybridizations from the two sets of three microarrays (phloem exudate and LMPC-derived tissue) was determined using density plots and boxplots at the Microarray Facility.

The results of the microarray hybridization experiments were then verified for 23 randomly selected genes, using real-time RT-PCR (Table 1). Among them were those that revealed a significant 'present' call ($P \le 0.01$) on all three microarrays, whereas others were either absent (−) or were present on only one or two of the microarrays (+/−). The hybridaization results was confirmed by real-time RT-PCR except for two phloem exudate transcripts (At1g09960, At5g03840) and seven LMPC-derived RNAs (AtCg00490, At5g09330, At4g31800, At2g14610, At1g75040, At1g70880, At1g09960, At4g22200). These were amplified in all (+) or some of the RNA samples (+/−), but gave no significant hybridization signal on the microarray. This discrepancy is most likely due to the very low transcript

Table 1 Verification of microarray data with phloem exudate and LMPC-derived transcripts by real-time quantitative RT-PCR

Gene ID	PSM	PSQ	LM	LQ	Function
AtCg00490	+	+	−	+/−	Large subunit of Rubisco
At3g56240	+	+	+	+	CCH (copper chaperone)
At5g56150	+	+	+	+	UBC30; ubiquitin-protein ligase
At2g30860	+	+	+	+	AtGSTF9 (glutathione-*S*-transferase 9)
At2g16600	+	+	+	+	ROC3 (rotamase CyP3)
At1g65980	+	+	+	+	TPX1 (thioredoxin-dependent peroxidase 1)
At4g35985	+	+	−	−	Senescence/dehydration-associated protein
At5g09330	+	+	+/−	+	ANAC082 (NAC domain transcription factor 82)
At4g34410	+	+	−	−	AP2 domain-containing transcription factor
At4g31800	+	+	−	+	WRKY18 (WRKY DNA-binding protein 18)
At1g80840	+	+	−	−	WRKY40 (WRKY DNA-binding protein 40)
At2g14610	+	+	−	+/−	PR1 (pathogenesis-related gene 1)
At1g75040	+	+	−	+/−	PR5 (pathogenesis-related gene 5)
At5g41990	+	+	−	−	WNK8 (Arabidopsis WNK kinase 8)
At1g70880	+/−	+/−	−	+/−	Bet v I allergen family protein
At1g22710	+/−	+/−	+	+	SUC2 (sucrose-proton-symporter 2)
At2g37330	+/−	+/−	+	+	ALS3 (aluminium-sensitive 3)
At1g09960	−	+/−	−	+	SUT4 (sucrose transporter 4)
At5g03840	−	+/−	−	−	TFL1 (terminal flower 1)
At5g17690	−	−	−	−	TFL2 (terminal flower 2)
At5g15840	−	−	−	−	CO (CONSTANS); transcription factor
At4g22200	−	−	−	+ (low)	AKT2 (Arabidopsis K$^+$ transporter 2)
At4g18290	−	−	−	−	KAT2 (K$^+$ Arabidopsis transporter 2)

(+), transcript detected; (−), transcript below the detection limit; (+/−), transcript was only detected in some samples.
PSM, phloem sap microarray; PSQ, quantitative RT-PCR of phloem sap; LM, LMPC microarray; LQ, quantitative RT-PCR of LMPC samples.

number and extremely high sensitivity of the real-time PCR. Those that were not detectable by quantitative RT-PCR revealed no measurable signal on the microarrays (Table 1, labeled with '−'). Thus, all transcripts with a significant 'present' call ($P ≤ 0.01$) on all three microarrays of the LMPC-derived samples were confirmed by real-time RT-PCR.

Furthermore, 20 out of 80 genes that are described as phloem-associated according to a search in the Arabidopsis Information Resource (TAIR) database (http://www.arabid opsis.org, March 2006) were present in the two phloem datasets (Table S1). They were significantly over-repre-sented ($P ≤ 0.01$, Fisher's exact test) within the group of phloem-annotated genes, substantiating the phloem origin of our RNA samples. In contrast, the six genes identified in our samples using the keyword 'xylem' were not signifi-cantly over-represented in the group of 47 xylem-annotated genes of the TAIR database.

Having confirmed the quality of the microarray data, only genes with hybridization signals that met the signif-icance criterion of a P-value $≤0.01$ on all three microarrays were referred to as present in the phloem sap or LMPC-derived phloem tissue (Table S2). According to this anal-ysis, 2417 transcripts were detected by microarrays in the phloem sap and 1291 in LMPC-derived phloem tissue of Arabidopsis. Among the 2417 mobile transcripts of the phloem exudates, 90 encode proteins potentially involved in signalling according to the pathway analysis program MapMan (Table 2). However, it might very well be that other phloem exudate transcripts also serve as mobile signals because they are translocated via the phloem stream to distant tissues and are translated there. The exudate transcripts and the 1291 LMPC-derived transcripts of phloem tissues were compared with a companion-cell EST (CC-EST) collection of Arabidopsis (444 transcripts). This EST library was previously generated from transcripts isolated in our laboratory from a pure companion-cell protoplast preparation (Ivashikina *et al.* 2003). The 114 transcripts that were present in all three datasets (Fig-ure 6), and thus were identified by three different tech-niques, very likely represent those that are specific for the phloem of Arabidopsis (Table S2). However, 1499 tran-scripts were only present in exudates and 433 were only present in LMPC-derived phloem tissue (Figure 6 and Table S2). Interestingly, the number of transcripts present in both CC-ESTs and LMPC-derived phloem tissue (90 transcripts), and those present in both CC-ESTs and phloem exudate (30 transcripts), were significantly over-represented in both microarray datasets (Table S2). The transcript number of CC-ESTs was more strongly over-represented in the LMPC-derived phloem tissue as in the phloem exudate. This indicates that not all transcripts of the companion cells are transported into the sieve tube. Nevertheless, this comparison suggests that more than

half of the 1291 transcripts found in LMPC-derived phloem tissue are mobile (714 + 114), as they are also present in the phloem sap. The differences in transcript mobility might be explained by the size-exclusion limit of plasmo-desmata. Some RNA molecules are too large or are associated with chaperones and therefore cannot pass through the plasmodesmata. Other RNA molecules might be degraded very fast or constantly associated with ribosomes due to high translational activity and therefore do not leave the companion cell.

In a further step, the pathway analysis program MapMan was used for functional categorization (version 2.1.1, Sep-tember 2007; http://gabi.rzpd.de/projects/MapMan/; Usadel *et al.*, 2005). The largest number of transcripts of the three datasets (phloem exudate, LMPC-derived phloem tissue and CC-ESTs) were found to fall into the functional categories 'protein', 'RNA' and 'stress', followed by 'transport' for exudate samples, 'photosynthesis' for LMPC-derived tissue, and 'hormone metabolism' for CC-EST samples (Figure S5). However, based on factorial changes, a statistical test for over- or under-representation of the transcript number of a functional category within its respective MapMan category revealed that the major category 'protein' was significantly over-represented in exudate and LMPC samples but not in CC-ESTs (Figure 7a,b). The 'stress' category was over-represented in exudate and CC-ESTs, and the second-largest category 'RNA' was significantly under-represented in exu-date and LMPC-derived samples (Figure 7b) and was not significant in CC-ESTs. However the categories 'mitochon-drial electron transport/ATP synthesis', 'photosynthesis', 'redox' and 'metal handling' were significantly over-repre-sented in all three phloem datasets (Figure 7a). In addition, sulfur assimilation and C_1 metabolism were significantly over-represented in exudate and LMPC-derived samples, but not in CC-ESTs (Figure 7a,b).

Discussion

In the study described here, phloem sap sampling and LMPC techniques were used to obtain pure Arabidopsis phloem transcripts that had been identified by genome-wide expression analysis using microarrays. In combination with advanced metabolite analyses such as CE-ESI-oTOF-MS for glucosinolates, we used a set of methods to identify mobile components in the phloem of *Arabidopsis thaliana*. An analysis of transcripts for previously published marker genes, as well as metabolite profiles for sieve element–companion cell complexes and phloem exudates, indicated that our samples contained non-detectable levels of contamination from adjacent tissues.

In order to test whether our phloem exudate transcript dataset can be used to identify mobile transcripts of the phloem in other microarray experiments with Arabidopsis plants or organs, we compared it with those obtained in

Gene ID	Description
Sugar and nutrient physiology	
At3g06483	Similar to mitochondrial pyruvate dehydrogenase kinase
At5g09440	Similar to *phi-1* (phosphate-induced gene)
At5g64260	Similar to *phi-1* (phosphate-induced gene)
Light	
At1g02340	Long hypocotyl in far-red phytochrome signaling 1 (HFR1)
At2g02950	Phytochrome kinase substrate 1 (PKS1)
At2g30520	Signal transducer of phototropic response (RPT2)
At3g26740	Similar to light-regulated protein
At3g45780	Non-phototropic hypocotyl protein 1 (NPH1)
At4g29080	Auxin-responsive protein 9 (IAA9)
At5g56280	COP9 signalosome subunit 6
Receptor kinases	
At2g31880	Leucine-rich repeat transmembrane protein kinase
At1g35710	Leucine-rich repeat transmembrane protein kinase
At1g07650	Leucine-rich repeat transmembrane protein kinase
At5g49760	Leucine-rich repeat family protein
At1g53440	Leucine-rich repeat family protein
At1g70530	Protein kinase family protein
At4g21400	Protein kinase family protein
At2g13790	Somatic embryogenesis receptor-like kinase 4 (AtSERK4)
At2g13800	Somatic embryogenesis receptor-like kinase 5 (AtSERK5)
At1g11280	S-locus protein kinase
At1g34300	Lectin protein kinase family protein
At4g27300	S-locus protein kinase
At1g21250	Identical to wall-associated kinase 1 (WAK1)
Calcium	
At5g01740	Wound-inducible protein
At1g09210	Calreticulin 2 (CRT2)
At1g18210	Calcium-binding EF-hand family protein
At1g53210	Calcium-binding EF-hand family protein
At4g27280	Calcium-binding EF-hand family protein
At1g64850	Calcium-binding EF-hand family protein
At1g76650	Calcium-binding EF-hand family protein
At5g54490	Calcium-binding EF-hand family protein
At2g44310	Calcium-binding EF-hand family protein
At2g46600	Calcium-binding protein
At2g26190	Calmodulin-binding family protein
At4g33050	Calmodulin-binding family protein
At5g40190	Calmodulin-binding family protein
At2g38800	Calmodulin-binding family protein
At2g41090	Calmodulin-like calcium-binding protein, 22 kDa (CaBP-22)
At2g41100	Calmodulin-like 5 (AtCAL5); touch 3 (TCH3)
At1g66410	Calmodulin-1/4 (CAM4)
At5g37780	Calmodulin-4 (CAM4)
At3g51920	Calmodulin-9 (CAM9)
At3g56800	Calmodulin-2/3/5 (CAM3)
At1g62480	Similar to vacuolar calcium-binding protein
At3g57330	Putative Ca^{2+}-ATPase (ACA11)
At4g23650	Putative calcium-dependent protein kinase
At4g34150	Putative calcium-dependent protein kinase
Phosphinositides	
At1g21920	Similar to phosphatidylinositol-4-phosphate 5-kinase
At3g08510	Phosphoinositide-specific phospholipase C (AtPLC2)
At5g58670	Phosphoinositide-specific phospholipase C (AtPLC1)
G-proteins	
At1g06400	GTP-binding protein (ARA2)
At3g54840	GTPase (ARA6)
At1g56330	GTP-binding protein (SAR1B)

Table 2 Transcripts of phloem exudates representing potential mobile signals

Table 2 (Continued)

Gene ID	Description
At4g02080	GTP-binding protein (SAR1A)
At1g48630	Similar to GTP-binding protein
At1g49300	Similar to GTP-binding protein
At1g52280	Similar to GTP-binding protein
At3g11730	Similar to GTP-binding protein
At3g16100	Similar to GTP-binding protein
At3g62560	Similar to GTP-binding protein
At4g17530	Similar to GTP-binding protein
At4g19640	Similar to GTP-binding protein
At4g39990	Similar to GTP-binding protein
At5g47200	Similar to GTP-binding protein
At5g59150	Similar to GTP-binding protein
At3g18820	Similar to GTP-binding protein
At4g34390	Similar to G-protein alpha subunit
At4g35750	Similar to Rho-GTPase-activating protein 1
At3g59920	GDP dissociation inhibitor AtGDI2
At3g60860	Similar to guanine nucleotide exchange factor
At4g17170	Rab2-like GTP-binding protein (RAB2)
At5g20010	GTP-binding nuclear protein RAN1
At5g20020	GTP-binding nuclear protein RAN2
At5g55190	GTP-binding nuclear protein RAN3
At5g45130	Ras-related GTP-binding protein RHA1
At5g58590	Similar to Ran binding proteins AtRANBP1a/1b
MAP kinases	
At4g29810	Mitogen-activated protein kinase kinase 2 (MKK2)
At1g73500	Mitogen-activated protein kinase kinase, putative MKK9
At2g01450	Mitogen-activated protein kinase, putative MPK17
At3g45640	Mitogen-activated protein kinase, putative MPK3
At4g01370	Mitogen-activated protein kinase, putative MPK4
14-3-3 proteins	
At4g09000	14-3-3 protein GF14 chi (GRF1)
At5g38480	14-3-3 protein GF14 psi (GRF3)
At1g35160	14-3-3 protein GF14 phi (GRF4)
At5g16050	14-3-3 protein GF14 upsilon (GRF5)
At5g10450	14-3-3 protein GF14 lambda (GRF6)
At3g02520	14-3-3 protein GF14 nu (GRF7)
At5g65430	14-3-3 protein GF14 kappa (GRF8)
At2g42590	14-3-3 protein GF14 mu (GRF9)
At1g22300	14-3-3 protein GF14 epsilon (GRF10)

Transcripts encoding potential signalling proteins were detected by microarrays (ATH1) in phloem exudates of *Arabidopsis thaliana* and sorted into functional categories according to MapMan (version 2.1.1, September 2007; http://gabi.rzpd.de/projects/MapMan/; Usadel *et al.*, 2005).

nutrient starvation (Table S3), hormone action (Table S4) and light signalling microarray experiments (Table S5). These datasets were selected because the phloem of higher plants plays a crucial role in nutrient distribution, coordination of developmental processes, and long-distance signalling. The phloem translocates signals from the shoot to the root in response to nutrient deprivation, which regulate root genes involved in solute acquisition and metabolite assimilation (Lappartient *et al.*, 1999; Liu *et al.*, 2005) or lead to alterations in the composition of phloem nutrients (Walter and DiFonzo, 2007). The phloem is also involved in the distribution of hormones that control development (Friml, 2003; Sauter *et al.*, 2001), as well as light signalling, which is perceived in leaves to entrain the circadian clock in photoperiodism and is translocated to the apical meristem to initiate flowering (An *et al.*, 2004; Ayre and Turgeon, 2004; Kobayashi and Weigel, 2007). The microarray datasets were derived from Genevestigator (version 3; http://www.genevestigator.ethz.ch/). Genes that were ≥3-fold upregulated (log$_2$ fold change 1.6) by the stimulus were sorted into functional categories using the pathway analysis program MapMan (Usadel *et al.*, 2005). A ≥3-fold cut-off was used to identify only strongly induced genes for comparison.
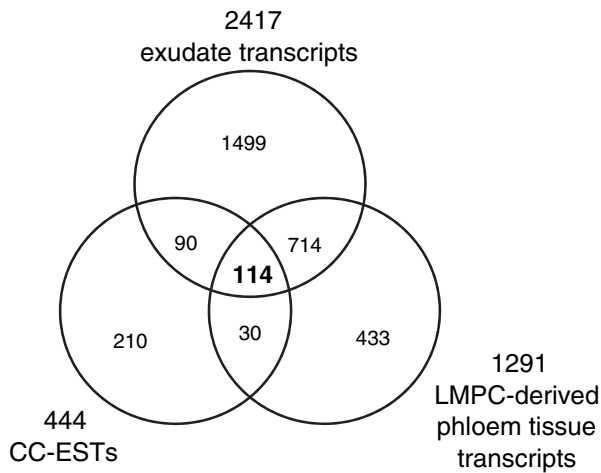
Figure 6. Intersection of Arabidopsis transcripts present in phloem exudate, phloem LMPC-derived sections and companion-cell ESTs (CC-ESTs).
The 444 ESTs listed by Ivashikina *et al.* (2003) were compared with 2417 transcripts present on microarrays hybridized with mRNA from three samples of phloem exudates or with 1291 transcripts from three LMPC-derived phloem tissue samples.

Nutrition

In microarray datasets of the Genevestigator database dealing with potassium, nitrate and sulfur starvation, 318 genes were induced under potassium depletion, of which 29 were present among 2417 transcripts of the phloem exudate (Figure S6/Table S6). Among them, five are related to stress, two are involved in calcium signalling, and one is a transcription factor. Recently, it has been shown that tolerance to low potassium is mediated via calcium sensors (Hedrich and Kudla, 2006). Two transcripts of EF-hand Ca^{2+}-binding genes were present in our phloem exudate transcript collection. They may signal the calcium status over long distances from one part of the plant to the other, as suggested for the proteins of this gene family (Lee *et al.*, 2004). Of the 404 genes identified as upregulated in response to low-nitrate conditions, 12 were phloem-related (Figure S6/Table S6). Among them were the transcripts of a peptide transporter and a purine transporter, a phospholipase A, a MAP kinase and two transcription factors. In addition to the two carriers for nitrogen-rich peptides and purines, a phloem-specific amino acid transporter and a cytokinin-permeable purine carrier have been described previously (Burkle *et al.*, 2003; Okumoto *et al.*, 2004). Three of the 38 genes upregulated during sulfur deprivation were present in the phloem (Figure S6/Table S6). These three genes, however, were classified as unknown by MapMan. A statistical analysis revealed that the exudate transcripts found in the nutrient starvation groups were not significant over-represented within the respective Genevestigator datasets (Table S3). This means that they could just as well be
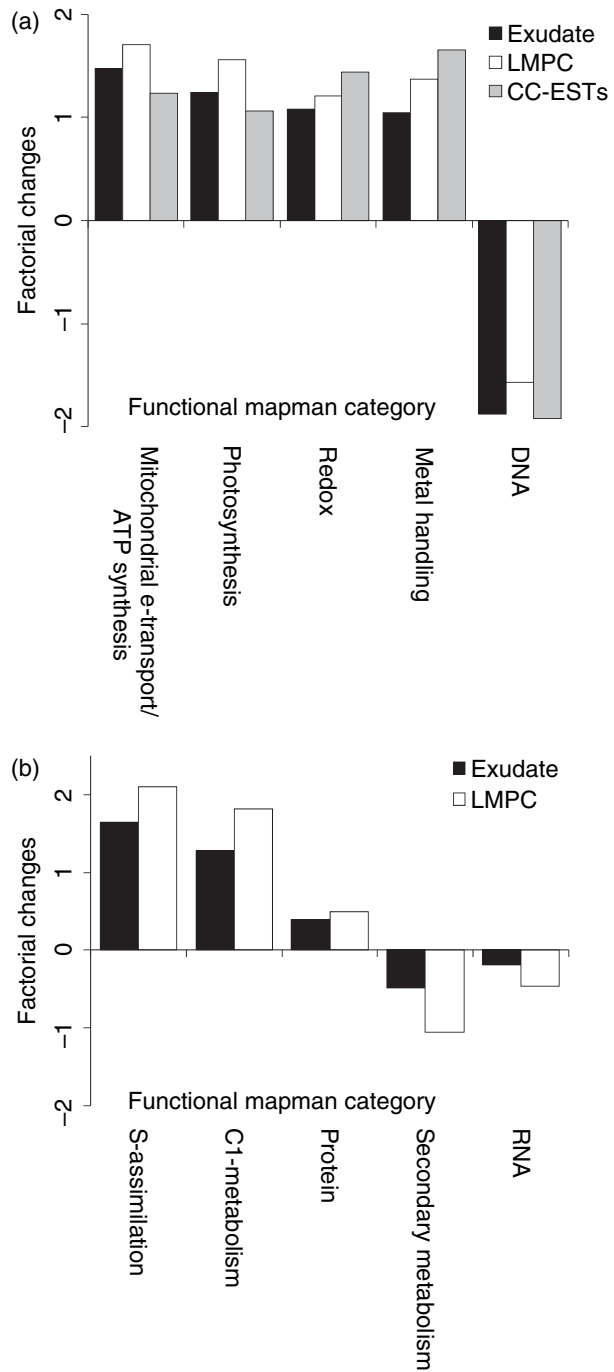
Figure 7. Factorial changes in functional categories of all genes that were present either in phloem exudate, LMPC-derived phloem tissues or companion-cell ESTs (CC-ESTs).
The natural logarithm (ln) of factorial changes is plotted against each functional MapMan category. Positive factorial changes indicate a larger number of genes in a functional category than expected and negative ones indicate a smaller number of genes in a functional category than expected from the total number of genes in the respective MapMan category. Functional categories that are significantly over- or under-represented (a) within all three phloem datasets, and (b) within exudate and LMPC-derived microarrays only.

randomly present in the phloem exudates. The result confirmed our expectations because the plants used for phloem sap collection were grown under normal nutrient conditions.

Hormones

The microarray gene expression data for three representatives of the classical plant hormones gibberellic acid (GA3), auxin (indole acetic acid, IAA) and cytokinin (zeatin) were also selected for comparison with phloem exudate transcripts. Gene collections of 207 GA3-, 56 IAA- and 175 zeatin-induced genes contained two, three and five transcripts, respectively, that were found in the phloem exudate (Figure S7/Table S7). One of the two GA3-sensitive genes found among the phloem transcripts is a protein kinase The three transcripts of the auxin dataset/exudate intersection encode the auxin-responsive protein, IAA2, a protein kinase and an EF-hand Ca^{2+}-binding factor. Among the five zeatin-activated genes was a regulator of transcription and one related to cell division. However, the number of transcripts of each of the phytohormone groups were not significantly over-represented within their Genevestigator class according to statistical analysis, meaning that they could be present just by chance in the exudate (Table S4). Whether the genes are involved in phloem development or signalling should now be tested.

Light

In order to identify the transcripts of light-sensitive genes in Arabidopsis phloem exudates, the genes from experiments using Arabidopsis seedlings treated with blue (BL), red (RL) and far-red light (FRL) were chosen for comparison. Among the 41 BL-, 33 RL- and 48 FRL-induced genes that intersected with transcripts of the phloem exudates (Figure S8/Table S8), 31 are shared by all three light regimes (Figure S9/Table S9). The major proportion of the 31 genes activated by all three light regimes belongs to the functional category 'photosynthesis/chloroplast'. Most interestingly, the transcripts of *phytochrome kinase substrate 1*, the signal transducer of phototropic response, *ROOT PHOTOTROPISM* (*RPT2*) and the APETALA2/ethylene-responsive element binding protein family (AP2/EREBP) appear to represent components of a phloem-distributed light-signalling system. In addition to this common gene set, we identified two RL-, three BL- and ten FRL-specific ones. The stimulus 'light' was the only one of the three stimuli chosen for which the number of genes in each group was significantly over-represented within their Genevestigator class (Table S5). This was strengthened by the fact that transcripts of the functional category 'photosynthesis' were also significantly over-represented within their functional MapMan category (Figure 7). The plants used for phloem sap collection were

grown in nutrient-rich soil and had just begun to flower; conditions that are reflected by the exudate transcript pattern found by the comparison outlined above.

Our phloem dataset can now be used to identify the genes in phloem- and cambium-enriched samples of Arabidopsis roots (Zhao *et al.*, 2005), poplar bark (Prassinos *et al.*, 2005), major veins of *Plantago* petioles (Pommerrenig *et al.*, 2006), the phloem transcriptome of *Apium graveolens* (Vilaine *et al.*, 2003) or *Brassica napus* (Giavalisco *et al.*, 2006), for example, as well as array experiments with whole Arabidopsis shoots (see examples above). It will now be possible to study the distribution of phloem-associated signals in response to various stimuli such as pathogen challenge and/or wounding. The phloem transcript sets assembled for this report represent a valuable resource for predicting new genes that are potential regulators of plant development and function. Questions regarding the molecular genetic nature of P-proteins and P-plastids, for example, may now be addressed (van Bel *et al.*, 2002). Examples of regulatory genes identified for this report include a number of uncharacterized genes for which roles in phloem action and the integration of phloem developmental processes have not yet been established.

Experimental procedures

Fixation and embedding of plant material

In our hands, fixation of Arabidopsis inflorescence stems using 3:1 ethanol : acetic acid (Kerk *et al.*, 2003; Yu *et al.*, 2007) resulted in low amounts of RNA. With 100% ethanol, however, the RNA yield was high, but preservation of the morphology required for sectioning with LMPC was poor. The best result was achieved by fixation overnight at 4°C with an ethanol:acetic acid ratio of 5:1. Following a standard solvent exchange procedure involving ethanol and Roticlear (Roth, http://www.carl-roth.de), the material was vacuum-infiltrated with low-melting-temperature wax (melting temperature 45°C, Plano, http://www.plano-em.de) using a self-made infiltration device (Figure S1).

Laser microdissection and pressure catapulting (LMPC)

In previous protocols, 10–20 μm LMPC sections were placed onto a water droplet on top of a membrane-coated LMPC slide and fixed at 40°C overnight. This, however, led to RNA wash-out into the water droplet (Cai and Lashbrook, 2006; Inada and Wildermuth, 2005), resulting in reduction of RNA yield of up to 90%. In order to avoid contact of specimens with water, we transferred the sections directly onto the slides by melting the paraffin at 60°C. Following de-paraffination five to seven times using Histoclear™ (National Diagnostics, http://www.nationaldiagnostics.com) and a twofold washing step with 100% ethanol, the RNA could be extracted. For control of RNA quality, fixed and complete cross-sections were scraped off the slide. Cross-sections on the slides used for microdissection were stained with toluidine blue-saturated ethanol and dried at 37°C. LMPC was carried out using the PALM MicroBeam system (PALM, http://www.palm-microlaser.

com). Approximately 100 phloem areals (approximately 200.000 μm^2) were catapulted into one reaction tube with 5 μl lysis binding buffer (100 m$_M$ Tris/HCl, 500 m$_M$ lithium-dodecyl-sulfate (LiCl), 10 m$_M$ EDTA, 1% LiDS, 5 m$_M$ DTT, pH 8) containing 1.2 units RNase inhibitor (MBI, http:www.fermantas.de). The material was collected at the bottom of the tube by brief centrifugation (14 000 **g**) and stored on ice until further processing. Approximately 25 tubes each of three independent experiments were used for RNA amplification.

Isolation and amplification of mRNA of LMPC-derived sections

The LMPC material collected on one day was pooled and the volume was adjusted to at least 100 μl with 1× lysis binding buffer (Dynal, http://www.invitrogen.com/site/us/en/home/brands/Dynal.html). mRNA was isolated using 15 μl Dynabeads$^{®}$ oligo (dT)$_{25}$ (Dynal) according to the manufacturer's instructions, and stored at −80°C. Purified mRNAs for each experiment were pooled, ethanol-precipitated in the presence of 0.03 vol linear acrylamide (Ambion, http://www.ambion.com), and re-dissolved in 3 μl di-ethylene pyrocarbonate (DEPC)-treated H_2O. All extraction and amplification steps (see below) were carried out using DNA/RNA low-binding tubes and tips (Eppendorf, http://www.eppendorf.de).

RNA amplification was based on the BD-SMART mRNA amplification kit (BD Biosciences, http://www.clontech.com). To pre-amplify full-length cDNAs prior to *in vitro* transcription, an additional 10-cycle PCR (95°C for 30 sec, 60°C for 1 min, 68°C for 10 min) was introduced using T7 extension and PCR primer II A of the kit. A maximum of 50 μg high-quality mRNA was amplified from 2 ng total RNA. An aliquot (approximately 10 ng of the amplified mRNA) was reverse-transcribed using M-MLV reverse transcriptase (Promega, http://www.promega.com/) and the resulting cDNA was tested using a LightCycler (Roche, http://www.roche.de) using primers for phloem marker transcripts as described previously (Ivashikina *et al.*, 2003). RNA integrity was monitored using a Bioanalyzer (Agilent) at the Microarray Facility, University of Tübingen, Germany (http://www.microarray-facility.com).

Preparation of phloem exudates and isolation of mRNA

Phloem exudates were obtained from adult rosette leaves at the start of flowering of approximately 10-week-old Arabidopsis plants (ecotype Col-0). Plants were cultivated in a Percival growth chamber (CLF Plant Climatics GmbH, http://www.plantclimatics.de) under short-day conditions (8 h light, 22°C/16 h dark, 16°C), illuminated with 100 μE of white light. Cut leaves were immediately transferred into the pre-incubation chamber of a home-made Plexiglas$^{®}$ device (Figure 4) containing EDTA buffer (5 m$_M$ Na$_2$EDTA, pH 7.5) osmotically adjusted to 270 mosmol with sorbitol. The petioles were re-cut under EDTA buffer in order to prevent sieve-tube embolism, and placed into the 3 mm gap of the pre-incubation chamber. Petiole fragments were removed and the pre-incubation chamber was washed by sucking 100 ml of EDTA buffer through the chamber using a 50 ml syringe. Approximately 3–4 ml EDTA buffer remained in the 3 mm gap, which was just enough to cover the cut ends of the petioles. Between 50 and 70 leaves were loaded for each experiment into the Plexiglas$^{®}$ device, illuminated (30 μE), and incubated at 25°C in CO_2- and H_2O-saturated air (1 l of 0.1 $_M$ NaHCO$_3$ per 0.05 m^3). After 1 h of bleeding, the EDTA buffer containing phloem exudate was removed using a 5 ml syringe, and samples were immediately frozen at −80°C. The EDTA buffer containing phloem exudate (3–4 ml) was lyophilized at −51°C (0.77 mbar) until a volume of approximately 100 μl remained (Christ Alpha 1-2, Hartenstein, http://www.martinchrist.de). mRNA was extracted using 15 μl Dynabeads$^{®}$ oligo(dT)$_{25}$ after addition of an equal volume of 2× lysis binding buffer according to manufacturer's instructions (Dynal).

Measurements of metabolites and minerals

Contents of amino acids and sugars were directly determined from phloem exudates in EDTA buffer. Amino acids were quantified using an amino acid analyzer (Biotronic LC5001, Eppendorf-Nethler-Hinz GmbH, http://www.eppendorf.de), sugars by HPLC (Dionex series 4500i chromatography system, Dionex, http://www1.dionex.com) and minerals by inductively coupled plasma (ICP) spectrometry (ICP-OES; JY70 Plus, Jobin Yvon, http://www.jobinyvon.de).

Real-time PCR

Control of abundance and quantification of actin and marker transcripts were performed by real-time PCR as described previously (Ivashikina *et al.*, 2003).

Microarray analysis

Microarray analyses were conducted at the Microarray Facility, University of Tübingen, Germany. RNA from four independent isolations was pooled and subjected to two rounds of linear amplification using the Affymetrix two-cycle cDNA synthesis kit (Affymetrix) according to the manufacturer's instructions. Briefly, 20 ng of RNA were reverse-transcribed using an oligo(dT) primer harbouring a T7 promoter sequence. The double-stranded cDNA was used as template in an *in vitro* transcription reaction. A second round of cDNA synthesis was performed using random hexamer primers. Second-strand synthesis was initiated with the oligodTT7 primer to facilitate a second round of *in vitro* transcription, thereby incorporating biotinylated UTP and CTP. The quality of the amplified cRNA was checked on a Bioanalyzer 2100 (Agilent). Labelled cRNA (20 μg) was fragmented and hybridized to Arabidopsis ATH1 GeneChip$^{®}$ arrays (Affymetrix) together with hybridization controls (two-cycle target labelling and control reagents; Affymetrix). After hybridization, the arrays were washed and stained in a Fluidics Station 450 (Affymetrix) with the recommended washing procedure. Biotinylated cRNA bound to target molecules was detected using streptavidin-coupled phycoerythrin, biotinylated anti-streptavidin IgG antibodies and streptavidin-coupled phycoerythrin again, according to the manufacturer's instructions. Microarrays were scanned using the GCS3000 GeneChip scanner (Affymetrix) and GCOS software, version 1.4. Scanned images were subjected to visual inspection to control for hybridization artefacts and proper grid alignment. The intensity files were analysed using Microarray Suite 5.0 (MAS5; Affymetrix) to generate report files for quality control and to calculate signal values for each probe set. All chips were scaled to an average signal value of 150 to enable comparison between individual microarrays. Each hybridization signal of a gene with a *P*-value ≤0.01 was classified as 'present' in the Arabidopsis phloem. Microarray data are provided in the MIAME standard public database GEO (http://www.ncbi.nlm.nih.gov/projects/geo/) with the series record GSE10247.

Functional categorization

The genes with a significant 'present' call ($P \leq 0.01$) in all three microarrays were sorted into functional categories according to the pathway analysis program MAPMAN (version 2.1.1, September 2007; http://gabi.rzpd.de/projects/MapMan/; Usadel *et al.*, 2005). To test the significance of over- or under-representation of the number of genes of a functional category in the respective MAPMAN category or the similarity with other datasets, Fisher's exact test was used. Factorial changes were determined to evaluate the over- or under-representation of a functional category within the MAPMAN category as described by Deeken *et al.* (2006). Functional categories of the phloem datasets with a positive factorial change have a higher proportion of genes than expected from the total number of genes assigned to that category. A negative value indicates a lower number of genes in the respective category than expected.

Comparison of phloem exudate transcripts with genes listed by Genevestigator

The 2417 phloem exudate transcripts were compared with other Affymetrix-derived microarray gene expression data published by Genevestigator (http://www.genevestigator.ethz.ch/). The BIO-MARKER SEARCH tool of Genevestigator was used in order to obtain a list of genes that were at least threefold upregulated in Arabidopsis upon nutrient depletion (potassium, sulfur, nitrate), phytohormone treatment (gibberellic acid 3, zeatin, IAA) or illumination with various light qualities (blue, red, far red). The treatment conditions of the Genevestigator experiments are outlined in Tables S3–S5.

CE-ESI-oTOF-MS determination of glucosinolates

The collected phloem exudates were lyophilized to dryness and resolved again in 100 μl of a standard solution containing 10 ng μl^{-1} sinigrin (Acros, http://www.acros.com). To analyse the chemical composition of phloem exudates from *Arabidopsis thaliana* with regard to glucosinolates, a recently developed CE-ESI-oTOF-MS method (Bringmann *et al.*, 2005) was used. The capillary electrophoresis (CE) experiments were performed on a Prince CE system (PrinCE Technologies, http://www.princetechnologies.eu) using a fused-silica capillary (Polymicro Technologies, http://www.polymicro.com) with 50 μm inner diameter and a length of 75 cm. Prior to use, the capillary was conditioned with 1 M NaOH; between the runs, it was rinsed with electrolyte consisting of 0.5 M aqueous formic acid. Due to the anodic separation, an electrospray ionization (ESI) potential of –20 kV, corresponding to 28 μA, was applied at the inlet. The capillary electrophoresis (CE) was coupled to a micrOTOF-Q (Bruker Daltonik, http://www.bdal.de), an orthogonally accelerated time-of-flight mass detector, by a grounded co-axial sheath liquid interface (Agilent). The sheath liquid, consisting of isopropanol:water (1:1 v/v) with 0.2% formic acid as an additive, was delivered by a syringe pump (Cole Palmer, http://www.colepalmer.com) at a flow rate of 4 μl min^{-1}. The micrOTOF-Q was operated with a nebulizer pressure of 0.15 bar, an ESI potential of +4.5 kV, and a mass range of *m/z* 50–1000. External calibration was performed using sodium formate clusters by switching the sheath liquid to a solution of 5 mM sodium hydroxide in the sheath-liquid system. An exact calibration curve was obtained based on the numerous cluster masses, each differing by 68 Da (NaCHO$_2$).

Supporting Information

Additional supporting information may be found in the online version of this article.

Please note: Blackwell Publishing are not responsible for the content or functionality of any supporting materials supplied by the authors. Any queries (other than missing material) should be directed to the corresponding author for the article.

Important note on changes in reproducible applicability of SMART cDNA synthesis from phloem tissue RNA of LMPC-derived samples

The Powerscript® reverse transcriptase (RT) is an essential component of the SMART mRNA amplification kit, originally distributed by BD/Clontech. This kit was commercially not available for a short period of time, because of a patent dispute between Takara Bio Inc. (Otsu, Shiga, Japan), the current owner of BD/Clontech and Invitrogen (Carlsbad, CA, USA). The SMART kit is now again available from Takara Bio Inc., but without Powerscript® RT. This SMART amplification kit functions properly with other RTs from different distributors when 200 ng of total RNA as recommended by Takara are used. However, amplification of high quality mRNA from

LMPC samples, equivalent to ≤2 ng of total RNA as gained with phloem sections in this study, was originally achieved with Power-script® RT, routinely, fails with any other RT, so far tested.

References

An, H., Roussot, C., Suarez-Lopez, P. *et al.* (2004) CONSTANS acts in the phloem to regulate a systemic signal that induces photo-periodic flowering of *Arabidopsis*. *Development*, **131**, 3615–3626.

Asano, T., Masumura, T., Kusano, H., Kikuchi, S., Kurita, A., Shimada, H. and Kadowaki, K.I. (2002) Construction of a specialized cDNA library from plant cells isolated by laser capture microdissection, toward comprehensive analysis of the genes expressed in the rice phloem. *Plant J.* **32**, 401–408.

Aung, K., Lin, S.I., Wu, C.C., Huang, Y.T., Su, C.L. and Chiou, T.J. (2006) pho2, a phosphate overaccumulator, is caused by a non-sense mutation in a microRNA399 target gene. *Plant Physiol.* **141**, 1000–1011.

Ayre, B.G. and Turgeon, R. (2004) Graft transmission of a floral stimulant derived from CONSTANS. *Plant Physiol.* **135**, 2271–2278.

van Bel, A.J., Ehlers, K. and Knoblauch, M. (2002) Sieve elements caught in the act. *Trends Plant Sci.* **7**, 126–132.

Bringmann, G., Kajahn, I., Neusüß, C., Pelzing, M., Laug, S., Unger, M. and Holzgrabe, U. (2005) Analysis of the glucosinolate pattern of *Arabidopsis thaliana* seeds by capillary zone electrophoresis coupled to electrospray ionization–mass spectrometry. *Electrophoresis*, **26**, 1513–1522.

Burkle, L., Cedzich, A., Dopke, C., Stransky, H., Okumoto, S., Gillissen, B., Kuhn, C. and Frommer, W.B. (2003) Transport of cytokinins mediated by purine transporters of the PUP family expressed in phloem, hydathodes, and pollen of *Arabidopsis*. *Plant J.* **34**, 13–26.

Cai, S. and Lashbrook, C.C. (2006) Laser capture microdissection of plant cells from tape-transferred paraffin sections promotes recovery of structurally intact RNA for global gene profiling. *Plant J.* **48**, 628–637.

Casson, S., Spencer, M., Walker, K. and Lindsey, K. (2005) Laser capture microdissection for the analysis of gene expression during embryogenesis of *Arabidopsis*. *Plant J.* **42**, 111–123.

Chen, S., Petersen, B.L., Olsen, C.E., Schulz, A. and Halkier, B.A. (2001) Long-distance phloem transport of glucosinolates in *Arabidopsis*. *Plant Physiol.* **127**, 194–201.

Corbesier, L., Vincent, C., Jang, S. *et al.* (2007) FT protein movement contributes to long-distance signalling in floral induction of *Arabidopsis*. *Science*, **316**, 1030–1033.

Deeken, R., Geiger, D., Fromm, J., Koroleva, O., Ache, P., Langenfeld-Heyser, R., Sauer, N., May, S.T. and Hedrich, R. (2002) Loss of the AKT2/3 potassium channel affects sugar loading into the phloem of *Arabidopsis*. *Planta*, **216**, 334–344.

Deeken, R., Engelmann, J.C., Efetova, M. *et al.* (2006) An integrated view of gene expression and solute profiles of *Arabidopsis* tumors: a genome-wide approach. *Plant Cell*, **18**, 3617–3634.

Friml, J. (2003) Auxin transport – shaping the plant. *Curr. Opin. Plant Biol.* **6**, 7–12.

Gentili, F. and Huss-Danell, K. (2003) Local and systemic effects of phosphorus and nitrogen on nodulation and nodule function in *Alnus incana*. *J. Exp. Bot.* **54**, 2757–2767.

Giavalisco, P., Kapitza, K., Kolasa, A., Buhtz, A. and Kehr, J. (2006) Towards the proteome of *Brassica napus* phloem sap. *Proteomics*, **6**, 896–909.

Haywood, V., Yu, T.S., Huang, N.C. and Lucas, W.J. (2005) Phloem long-distance trafficking of GIBBERELLIC ACID-INSENSITIVE RNA regulates leaf development. *Plant J.* **42**, 49–68.

Hedrich, R. and Kudla, J. (2006) Calcium signalling networks channel plant K$^+$ uptake. *Cell*, **125**, 1221–1223.

Husebye, H., Chadchawan, S., Winge, P., Thangstad, O.P. and Bones, A.M. (2002) Guard cell- and phloem idioblast-specific expression of thioglucoside glucohydrolase 1 (myrosinase) in *Arabidopsis*. *Plant Physiol.* **128**, 1180–1188.

Imlau, A., Truernit, E. and Sauer, N. (1999) Cell-to-cell and long-distance trafficking of the green fluorescent protein in the phloem and symplastic unloading of the protein into sink tissues. *Plant Cell*, **11**, 309–322.

Inada, N. and Wildermuth, M.C. (2005) Novel tissue preparation method and cell-specific marker for laser microdissection of *Arabidopsis* mature leaf. *Planta*, **221**, 9–16.

Ivashikina, N., Deeken, R., Ache, P., Kranz, E., Pommerrenig, B., Sauer, N. and Hedrich, R. (2003) Isolation of AtSUC2 promoter–GFP-marked companion cells for patch–clamp studies and expression profiling. *Plant J.* **36**, 931–945.

Karley, A.J., Douglas, A.E. and Parker, W.E. (2002) Amino acid composition and nutritional quality of potato leaf phloem sap for aphids. *J. Exp. Biol.* **205**, 3009–3018.

Kehr, J. and Buhtz, A. (2008) Long-distance transport and movement of RNA through the phloem. *J. Exp. Bot.* **59**, 85–92.

Kerk, N.M., Ceserani, T., Tausta, S.L., Sussex, I.M. and Nelson, T.M. (2003) Laser capture microdissection of cells from plant tissues. *Plant Physiol.* **132**, 27–35.

Kobayashi, Y. and Weigel, D. (2007) Move on up, it's time for change – mobile signals controlling photoperiod-dependent flowering. *Genes Dev.* **21**, 2371–2384.

Koroleva, O.A., Davies, A., Deeken, R., Thorpe, M.R., Tomos, A.D. and Hedrich, R. (2000) Identification of a new glucosinolate-rich cell type in *Arabidopsis* flower stalk. *Plant Physiol.* **124**, 599–608.

Lappartient, A.G., Vidmar, J.J., Leustek, T., Glass, A.D. and Touraine, B. (1999) Inter-organ signalling in plants: regulation of ATP sulfurylase and sulfate transporter genes expression in roots mediated by phloem-translocated compound. *Plant J.* **18**, 89–95.

Lee, S., Lee, E.J., Yang, E.J., Lee, J.E., Park, A.R., Song, W.H. and Park, O. K. (2004) Proteomic identification of annexins, calcium-dependent membrane binding proteins that mediate osmotic stress and abscisic acid signal transduction in *Arabidopsis*. *Plant Cell*, **16**, 1378–1391.

Li, C., Zhao, J., Jiang, H., Wu, X., Sun, J., Zhang, C., Wang, X., Lou, Y. and Li, C. (2006) The wound response mutant suppressor of prosystemin-mediated responses 6 (spr6) is a weak allele of the tomato homolog of CORONATINE-INSENSITIVE 1 (COI1). *Plant Cell Physiol.* **47**, 653–663.

Liu, J., Samac, D.A., Bucciarelli, B., Allan, D.L. and Vance, C.P. (2005) Signalling of phosphorus deficiency-induced gene expression in white lupin requires sugar and phloem transport. *Plant J.* **41**, 257–268.

Lohaus, G., Hussmann, M., Pennewiss, K., Schneider, H., Zhu, J.J. and Sattelmacher, B. (2000) Solute balance of a maize (*Zea mays* L.) source leaf as affected by salt treatment with special emphasis on phloem retranslocation and ion leaching. *J. Exp. Bot.* **51**, 1721–1732.

Lough, T.J. and Lucas, W.J. (2006) Integrative plant biology: role of phloem long-distance macromolecular trafficking. *Annu. Rev. Plant Biol.* **57**, 203–232.

Lucas, W.J., Yoo, B.-C. and Kragler, F. (2001) RNA as a long-distance information macromolecule in plants. *Nat. Rev. Mol. Cell Biol.* **2**, 849–857.

Marten, I., Hoth, S., Deeken, R., Ache, P., Ketchum, K.A., Hoshi, T. and Hedrich, R. (1999) AKT3, a phloem-localized K$^+$ channel, is blocked by protons. *Proc. Natl Acad. Sci. USA*, **96**, 7581–7586.

Mathieu, J., Warthmann, N., Kuttner, F. and Schmid, M. (2007) Export of FT protein from phloem companion cells is sufficient for floral induction in *Arabidopsis*. *Curr. Biol.* **17**, 1055–1060.

Mewis, I., Appel, H.M., Hom, A., Raina, R. and Schultz, J.C. (2005) Major signalling pathways modulate *Arabidopsis* glucosinolate accumulation and response to both phloem-feeding and chewing insects. *Plant Physiol.* **138**, 1149–1162.

Mira, H., Martinez-Garcia, F. and Penarrubia, L. (2001) Evidence for the plant-specific intercellular transport of the *Arabidopsis* copper chaperone CCH. *Plant J.* **25**, 521–528.

Nakazono, M., Qiu, F., Borsuk, L.A. and Schnable, P.S. (2003) Laser-capture microdissection, a tool for the global analysis of gene expression in specific plant cell types, identification of genes expressed differentially in epidermal cells or vascular tissues of maize. *Plant Cell*, **15**, 583–596.

Nishimura, R., Hayashi, M., Wu, G.J. *et al.* (2002) HAR1 mediates systemic regulation of symbiotic organ development. *Nature*, **420**, 426–429.

Okumoto, S., Koch, W., Tegeder, M., Fischer, W.N., Biehl, A., Leister, D., Stierhof, Y.D. and Frommer, W.B. (2004) Root phloem-specific expression of the plasma membrane amino acid proton co-transporter AAP3. *J. Exp. Bot.* **55**, 2155–2168.

Olsson, J.E., Nakao, P., Bohlool, B.B. and Gresshoff, P.M. (1989) Lack of systemic suppression of nodulation in split root systems of supernodulating soybean (*Glycine max* [L.] Merr.) mutants. *Plant Physiol.* **90**, 1347–1352.

Oparka, K.J. (ed.) (2005) *Plasmodesmata*. Blackwell Scientific Publishing, Oxford.

Pommerrenig, B., Barth, I., Niedermeier, M., Kopp, S., Schmid, J., Dwyer, R.A., McNair, R.J., Klebl, F. and Sauer, N. (2006) Common plantain. A collection of expressed sequence tags from vascular tissue and a simple and efficient transformation method. *Plant Physiol.* **142**, 1427–1441.

Pommerrenig, B., Papini-Terzi, F.S. and Sauer, N. (2007) Differential regulation of sorbitol and sucrose loading into the phloem of *Plantago major* in response to salt stress. *Plant Physiol.* **144**, 1029–1038.

Prassinos, C., Ko, J.H., Yang, J. and Han, K.H. (2005) Transcriptome profiling of vertical stem segments provides insights into the genetic regulation of secondary growth in hybrid aspen trees. *Plant Cell Physiol.* **46**, 1213–1225.

Sauter, A., Davies, W.J. and Hartung, W. (2001) The long-distance abscisic acid signal in the droughted plant: the fate of the hormone on its way from root to shoot. *J. Exp. Bot.* **52**, 1991–1997.

Turnbull, C.G., Booker, J.P. and Leyser, H.M. (2002) Micrografting techniques for testing long-distance signalling in *Arabidopsis*. *Plant J.* **32**, 255–262.

Usadel, B., Nagel, A., Thimm, O. *et al.* (2005) Extension of the visualization tool MapMan to allow statistical analysis of arrays, display of corresponding genes, and comparison with known responses. *Plant Physiol.* **138**, 1195–1204.

Vilaine, F., Palauqui, J.C., Amselem, J., Kusiak, C., Lemoine, R. and Dinant, S. (2003) Towards deciphering phloem: a transcriptome analysis of the phloem of *Apium graveolens*. *Plant J.* **36**, 67–81.

Walter, A.J. and DiFonzo, C.D. (2007) Soil potassium deficiency affects soybean phloem nitrogen and soybean aphid populations. *Environ. Entomol.* **36**, 26–33.

Walz, C., Giavalisco, P., Schad, M., Juenger, M., Klose, J. and Kehr, J. (2004) Proteomics of curcurbit phloem exudate reveals a network of defence proteins. *Phytochemistry*, **65**, 1795–1804.

Wolf, O., Munns, R., Tonnet, M.L. and Jeschke, W.D. (1990) Concentrations and transport of solutes in xylem and phloem along the leaf axis of NaCl-treated *Hordeum vulgare*. *J. Exp. Bot.* **41**, 1133–1141.

Yoo, B.C., Kragler, F., Varkonyi-Gasic, E., Haywood, V., Archer-Evans, S., Lee, Y.M., Lough, T.J. and Lucas, W.J. (2004) A systemic small RNA signalling system in plants. *Plant Cell*, **16**, 1979–2000.

Yu, Y., Lashbrook, C.C. and Hannapel, D.J. (2007) Tissue integrity and RNA quality of laser microdissected phloem of potato. *Planta*, **226**, 797–803.

Zhao, C., Craig, J.C., Petzold, H.E., Dickerman, A.W. and Beers, E.P. (2005) The xylem and phloem transcriptomes from secondary tissues of the *Arabidopsis* root-hypocotyl. *Plant Physiol.* **138**, 803–818.